Tellus (2003), 55B, 145–158
Printed in UK. All rights reserved

TELLUS
ISSN 0280–6509

The impact of local winds and long-range transport on the continuous carbon dioxide record at Mount Waliguan, China

By LINGXI ZHOU[1,2]*, JIE TANG[1], YUPU WEN[1], JINLONG LI[3], PENG YAN[1] and XIAOCHUN ZHANG[4],
[1]*Chinese Academy of Meteorological Sciences, Beijing 100081, China;* [2]*National Institute for Environmental Studies, Tsukuba, Ibaraki 305-0053, Japan;* [3]*Center of Environmental Sciences, Peking University, Beijing 100871, China;* [4]*Qinghai Meteorological Bureau, Xining 810001, Qinghai Province, China*

(Manuscript received 2 January 2002; in final form 16 December 2002)

ABSTRACT

This paper describes the continuous measurements of atmospheric carbon dioxide at Mt. Waliguan (36°17′N, 100°54′E, 3816 m asl) in western China over the period 1994–2000. The CO_2 hourly mixing ratios were segregated by horizontal wind direction/speed and vertical winds, respectively, merged by season over the entire measurement period. The short-term variability in CO_2 was examined mainly from the point of view of local winds observed at this station and isobaric back trajectory cluster-concentration analysis as for local and long-range transport influence, to permit the selection of hourly average data that is representative of background conditions. From the selected hourly data, daily, monthly and annual averages that are not influenced by local CO_2 sources and sinks be computed by discriminating the local and regional impact on the Waliguan CO_2 records. On the basis of these results, background CO_2 data were then analyzed to evaluate the averaged diurnal variation, monthly mean time series, CO_2 mixing ratio distribution in different seasons as well as averaged seasonal cycle. Annual mean and growth rate of CO_2 at Waliguan during the period of 1991 to 2000 were further discussed by supplement with NOAA/CMDL flask air sampling records at this station and other monitoring stations located at similar latitudinal band in the Northern Hemisphere. The results from this study can provide atmospheric CO_2 characteristics in Asian inland regions, and be used in other studies to improve the understanding of carbon source and sink distributions.

1. Introduction

Long-term observation of carbon dioxide (CO_2) mixing ratios in the atmosphere have provided a basis for studies of the global carbon cycle and CO_2-induced climatic change. The atmospheric burden of CO_2 has been monitored at many sites world-wide for many years (Conway and Steele, 1989; Conway et al., 1994; Keeling et al., 1976a, b; Tans et al., 2001; WMO, 1981; 2000). Waliguan Observatory, located at the remote area of western China, is one of the World Meteorological Organization (WMO)'s 22 Global Atmosphere Watch (GAW) Baseline Stations scattered around the world (Wen et al., 1994; WMO, 1978; 1993; 1997; Zhou et al., 1998a, b). Figure 1 shows the geographical distribution of the 22 stations (http://www.wmo.ch/web/gcos/gif/gaw.gif). The Waliguan station was established in 1994 and is situated in an important geographical region within the WMO-GAW's monitoring network providing

*Corresponding author: (JSPS Fellow, during March 2002–March2004), Center for Global Environmental Research, National Institute for Environmental Studies, 16-2 Onogawa, Tsukuba, Ibaraki 305-0053, Japan.
e-mail: zhou.lingxi@nies.go.jp
Permanent address: Research Center for Earth Environment and Global Change, Chinese Academy of Meteorological Sciences (CAMS), 46 Zhong-guan-cun South Street, Beijing 100081, P. R. China.
e-mail: zhoulx@cams.cma.gov.cn

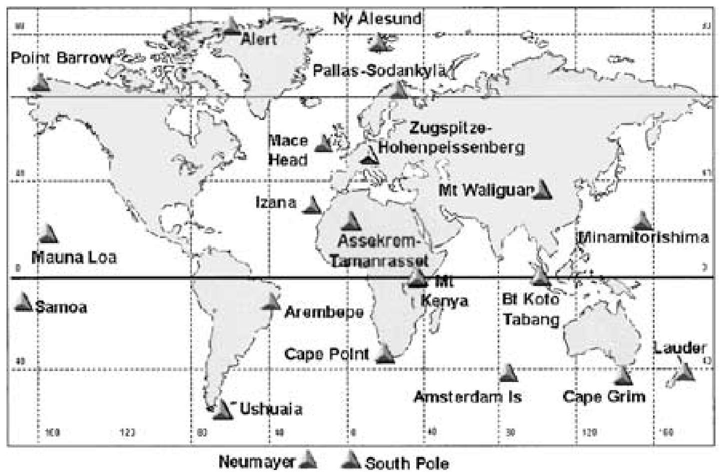

Fig. 1. Geographical distribution of the 22 baseline observatories in the WMO-GAW monitoring network (http://www.wmo.ch/web/gcos/gif/gaw.gif).

important information from the Eurasia continent. The overall measurement program includes a wide variety of typical baseline measurements, but with an emphasis on greenhouse gases and atmospheric ozone (Tang et al., 1995; Zhou et al., 1998a). Due to its unique location, large geographic region, multitude of measurements and the site's representativeness, the continuous atmospheric measurements from the Waliguan Observatory received increasing attention in recent years (Tans et al., 2001; Masarie and Tans, 1995; WMO, 2000; 2001).

Continuous measurements of CO_2 can provide great detail for the study of CO_2 variability and on its sources and sinks. Different researchers around the world have used various methods for filtering the observed CO_2 data, according to site location and environment (Bacastow et al., 1985; Beardsmore and Pearman, 1987; Ciattaglia, 1983; Ciattaglia et al., 1987; 1999; Gaudry et al., 1983; 1991; Halter et al., 1988; Halter and Harris, 1983; Harris and Kahl, 1990; Harris, 1992; Haszpra, 1999; Keeling et al., 1976a, b; Navascues and Rus, 1991; Thoning et al., 1989; Watanabe et al., 2000; Waterman et al., 1989). The typical CO_2 background data selection that is utilized at many other remote site locations has been applied to the Waliguan CO_2 data (Wen et al., 1994) up to now. This has been shown to be suitable for some ocean and polar stations that have relatively uniform wind direction for sustained periods, but is not suitable for Waliguan due to its meteorological, landform and environmental conditions.

In this paper we will examine the short-term variability in CO_2 of one day or less to permit the selection of hourly average data that are representative of background conditions. From these selected data, daily, monthly and annual averages that are not influenced by local CO_2 sources and sinks be computed by discriminating the local and regional impact on the Waliguan CO_2. It can provide the thorough understanding of atmospheric CO_2 background variations and the major influencing factors in the inland plateau of China, and provide long-term, continuous and accurate observation records for the use in global climate and other related research activities. It can also provide the CO_2 background values to determine the behavior of the Asian mainland on a global scale, and further interpret the formation of CO_2 background characteristics over continental Asia.

2. Site and experiment

Figure 2 shows the topographical distribution of the area within 100 km around Mt. Waliguan. Located at the edge of the north-eastern part of the Tibetan Plateau, the surrounding area primarily maintains its natural environment of sparse vegetation, with arid/semi-arid grassland and desert predominating. Yak and sheep pasturage is the main activity in summer with a small agricultural area in the lower valley. The population density is less than 6 people km^{-2} and relatively isolated from industry and

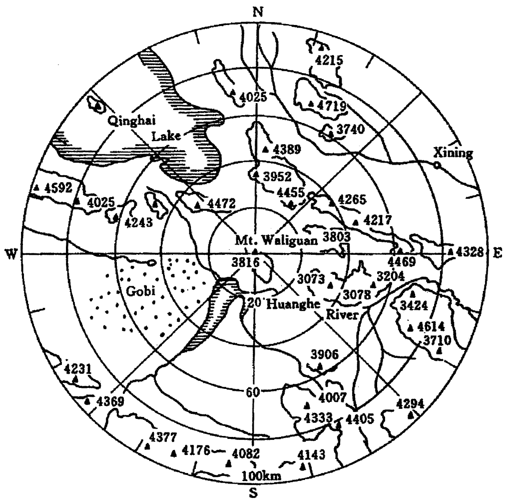

Fig. 2. Topographical map of Mt. Waliguan surrounding area within 100 km distance: triangles represent high mountains (height in m above sea level); scattered dots in the western part indicate desert area.

populated areas. The main building accommodating the in-situ CO_2 measurement systems, as well as a 89 m height triangular steel tower for the ambient air sampling and meteorological equipment (10, 20, 40 and 80 m height, respectively) for surface wind observation, are located at the top of Mt. Waliguan.

Atmospheric CO_2 is measured using a Licor6251 non-dispersive infrared (NDIR) analyzer, and a HP5890 gas chromatograph equipped with a flame ionization detector (GC-FID). Both systems are located in a second-floor laboratory. Ambient air is supplied via 3/8″ o.d. Dekoron® tubing extending 80 m up the tower, approximately 5 m away from the laboratory. Air is drawn in via vacuum pumps through pressure release valves set at 15 psi to remove excess air and allow high continuous flow through the main line (a Cole-Parmet Air Cadet model 7530-50 pump for the NDIR analyzer, sample flow 100 mL min^{-1}, an UN022 ANT KNF Neuberger pump for the GC-FID, sample flow 225 mL min^{-1}), and passes through a 7 μm in-line filter to remove particulate matter. The ambient air residence time from the top of the tower to the NDIR analyzer and GC-FID is about 30 s. The air flow then passes through glass traps submerged in methanol cryocoolers set at –52° (two series glass traps for the NDIR analyzer) and –70° (one glass trap for the GC-FID), respectively, to remove residual moisture.

Standard gases are supplied from pressurized 30 L treated aluminium alloy cylinders fitted with stainless-steel two-stage gas regulators. A group of five station standards C1 (339.31 ppmv CO_2 in clean dry air), C2 (347.02 ppmv), C3 (359.55 ppmv), C4 (371.84 ppmv) and C5 (379.73 ppmv), as well as reference tanks W1, W2, Zero and Target, are supplied to the NDIR system. The station standards were prepared and calibrated for CO_2 on an NDIR analyzer at the NOAA/CMDL laboratory. A group of three station standards CA01082 (331.81 ppmv CO_2 in clean dry air), CA01465 (347.22 ppmv) and CA01462 (354.45 ppmv), as well as two working standards AES034 and AES067, are supplied to the GC-FID system. The station standards were prepared by Praxair Inc. and calibrated for CO_2 on an NDIR system at the AES (MSC) laboratory in Toronto, Canada. The stabilities of all the standard gases are acceptable, with an absolute deviation less than 0.02 ppmv in the re-calibration activities carried out on the Waliguan NDIR system every half a year, as well as in the WMO round-robin CO_2 inter-comparison activities (Peterson, 1999).

The NDIR system began in November 1994 with an ambient analysis frequency of 1 min^{-1}. The GC-FID system began in July 1994 with an ambient analysis frequency of 3 injections h^{-1} (CO_2 converted to CH_4 by a heated nickel catalyst tube at 350 °C: the estimated reduction efficiency from CO_2 to CH_4 is around 90%). The estimated overall precisions of the NDIR and GC-FID analyses is below 0.02% and 0.05%, respectively, for an approximately 365 ppmv standard gas repeated injection (Wen et al., 1994; Zhou et al., 1998a). The surface wind observations began in July 1994; with a sampling frequency of once per 2 s, by an RMY-05103 wind monitor (R. M. Young Co.) for 10, 20, 40 and 80 m height horizontal wind speed and direction, and by an RMY-27106T anemometer for 80 m height vertical winds. The meteorological parameters are recorded on a CSI-21X Datalogger.

3. Results and discusion

3.1. Data handling

Ambient CO_2 hourly averages and standard deviations were derived from NDIR and GC-FID raw records. The two data sets were merged (Zhou et al., 1998a; Zhou, 2001) in order to reduce the data gap. Figure 3 is a box-whisker plot with estimated long-term trends, describing the time-series data for all the CO_2 hourly records from 1994 to 2000 obtained from

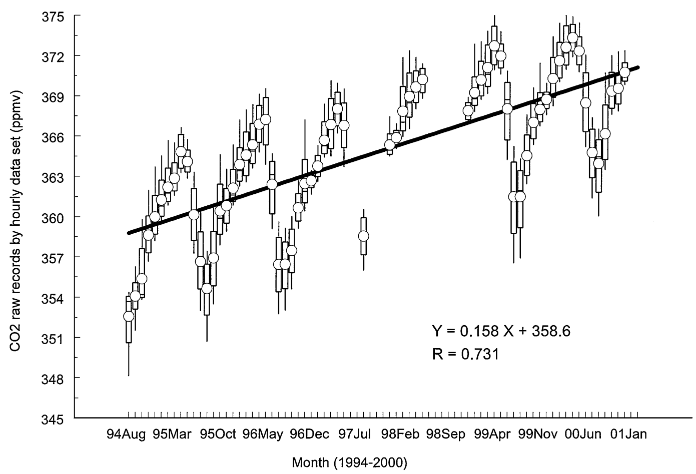

Fig. 3. Box-whisker plot (5%, 25%, median, 75% and 95%, open circles indicate averages) of CO_2 monthly mean time series as well as estimated linear trend, based on raw hourly records at Mt. Waliguan, 1994–2000.

the NDIR and GC-FID raw data at Mt. Waliguan. In order to realize the averaged statistical feature and its relationship in different seasons, estimated CO_2 long-term trends during 1994–2000 (a linear curve fit $Y = 0.158X + 358.6$ in Fig. 3) were removed. The detrended CO_2 hourly means were further deseasoned for the study of the short-term variation by subtract estimated corresponding monthly means (open circles in Fig. 3). A CO_2 value of 360 ppmv was added to each hourly mean residual (detrended and deseasoned) for the purpose of convenient plotting. The surface wind hourly records came from calculations on the raw data. Ambient CO_2 and surface wind hourly means were then partitioned corresponding to different seasons (March–May as spring, June–August as summer, September–November as autumn, December–February as winter). The impact of local winds and long-range transport on the observed CO_2 hourly records were further investigated mainly based on these partitioned data sets.

3.2. *Impact of local surface winds on the observed CO_2 hourly averages*

The annual prevailing wind directions at Mt. Waliguan are NW–W–WSW–SW (occurrence 55%, mostly in winter), and NE–ENE–E–ESE (about 40%, mostly in summer), with calm conditions occurring less than 4% of the time (Zhou, 2001). The wind roses in spring and autumn are similar, with a dominating SW–WSW–W and ENE–E–ESE, whereas the wind pattern in summer is dominated by an ENE–E–ESE and N pattern, and in winter by a SW–WSW–W–WNW pattern, as shown in Fig. 4. The CO_2 hourly mixing ratio was segregated by horizontal wind direction merged by season over the entire measurement period, as shown in Fig. 5. The results show that the horizontal wind direction of NE–ENE in summer contributes to an approximately 1.5 ppmv decline in CO_2 concentration, while in other seasons there is a rise of 1–2.5 ppmv. The situation is similar for the widening section of NNE–NE–ENE–E–ESE–SE–SSE.

Figure 6 illustrates the CO_2 mixing ratios weighted by the frequency of wind occurrence. This method of weighing (Gras, 2001) is a means of showing the relative importance of different local wind directions to the annual atmospheric CO_2 loading at Waliguan. As is evident in Fig. 6, in spring, autumn and winter the largest contributions originate from ENE and the contribution from W–WSW is the lowest, showing calm conditions have a small positive contribution. In summer, however, this pattern is reversed in that the NE–ENE sector has a large negative contribution to the CO_2 concentration level, while N has only a minimal positive contribution, and calm has a small negative contribution.

In winter, the temporal variability of CO_2, CH_4, BC (black carbon) and CO at Waliguan has been shown be similar even on timescales of less than a day (Zhou, 2001). BC and CO mainly produced by the combustion of carbonaceous material, such as fossil fuels and biomass (Conway et al., 1993; Hansen et al., 1989;

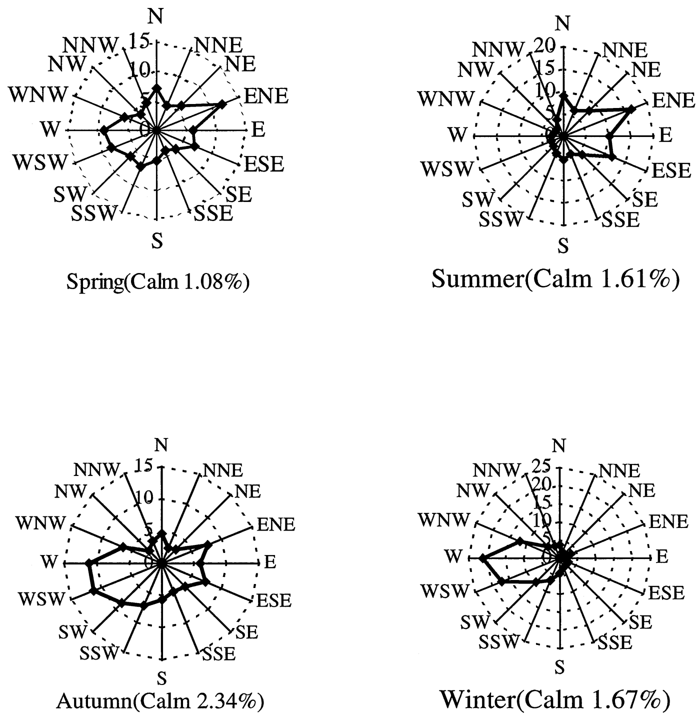

Fig. 4. Wind rose in spring, summer, autumn and winter at Mt. Waliguan, during the period 1994–2000.

Hopper et al., 1994). Since Waliguan is located in a drought temperate climatic zone surrounded primarily with low grasslands and mountainous regions, contributions from natural combustion sources such as forest fires would be negligible. CO_2 and CH_4 have significant biological sources, but again these processes would be minimal during the winter months. Using this simple argument, it is reasonable to conclude that the origin of Waliguan episodic increases in BC, CO, CO_2 and CH_4 is anthropogenic during winter. Since CO_2 has a relatively simple source/sink process, and combining the relationship of BC and CO concentration level with the surface wind direction and long-rang transport in different seasons, the highest BC and CO concentration in all seasons mainly happened in the NNE–NE and the adjacent direction, attributable to the large-scale emission and transport from the Yellow River Canyon industrial area in north-eastern region approximately 500 km away from Waliguan (Tang et al., 1999; Zhou et al., 2001). The lower CO_2 concentration level in the NE–ENE sector in summer is likely attributed to decreased anthropogenic emissions (heating activities, etc.) and increased photosynthesis (the major growing season in western China), due to a large vegetation distribution in this sector. The higher CO_2 level for the ENE direction in the other seasons is likely due to the elevated anthropogenic emission sources in this sector.

Horizontal wind speeds were divided by groups of <0.5, 0.5–3, 3–6, 6–10 and >10 m s^{-1}. The cases of wind speed <0.5 or >10 m s^{-1} in total account for approximately 10% occurrence in different seasons (Zhou et al., 2001). CO_2 averaged mixing ratios as a function of wind speed indicate that horizontal wind speed has a varying influence on the CO_2 concentration levels in different seasons. CO_2 level decreases with increasing wind speed by an alteration of up to 1.0 ppmv in spring and 1.5 ppmv in winter. The alteration, however, is less than 0.3 ppmv in summer or autumn. Calm conditions have a small positive contribution to the CO_2 level in spring, autumn and winter; however, they have a small negative contribution to the CO_2 level in summer. In general, horizontal wind speed >10 m s^{-1} or calm conditions in all seasons has maximum impact on the CO_2 hourly mixing ratios at Waliguan.

Vertical winds were divided by groups of < -1, 1 to -0.3, -0.3 to 0.3, 0.3–1 and >1 m s^{-1} (where represent a downslope airflow). The circumstances of

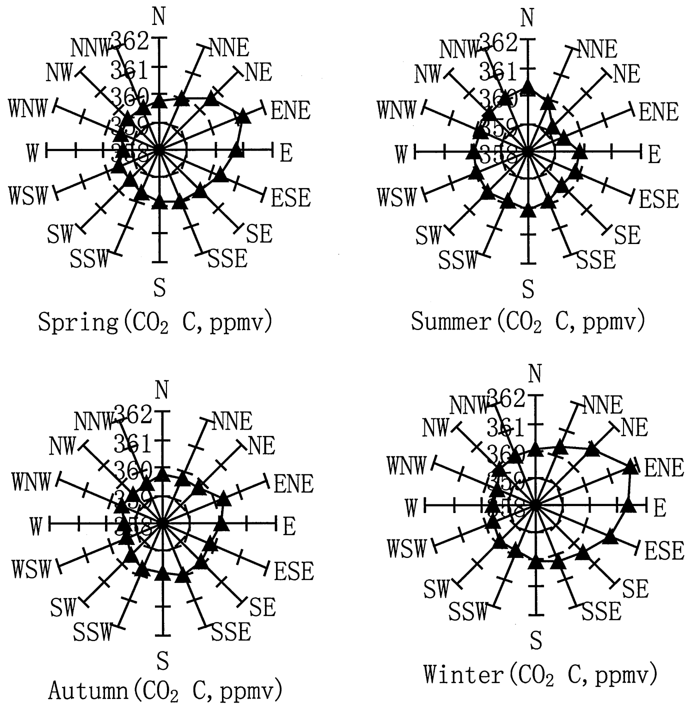

Fig. 5. CO_2 hourly mixing ratios segregated by horizontal wind direction merged by spring, summer, autumn and winter at Mt. Waliguan, 1994–2000.

vertical wind speed > ±1 m s^{-1} in total account for <10% occurrence in different seasons. Usually, as a result of local landform influence, horizontal winds from east of the sampling site bring a downslope airflow: horizontal winds from west of the sampling site, however, bring an upslope airflow (Zhou et al., 2001). The corresponding CO_2 mixing ratios show a slight decrease along with the upslope winds but show a small increase along with the downslope winds, coinciding with the above-cited statistical relationship between CO_2 mixing ratio and horizontal wind direction in different seasons. Generally, vertical wind speed >±1 m s^{-1} in all seasons has considerable impact on observed CO_2 hourly mixing ratios, depending on the different origin and route of air flow arriving at the Waliguan sampling site.

3.3. *Atmospheric CO_2 background data selection procedures*

Determining "baseline" conditions is necessary to minimize the effect of local sources and sinks of CO_2 on the long-term variations in the data series (Thoning et al., 1989; WMO, 2001). The procedure to select CO_2 hourly data representative of "baseline" conditions at Waliguan is as follows: (a)Remove CO_2 hourly averages with standard deviations (std) >1.0 ppmv (approximately 3% of the raw records removed); distinguish the visible instrument fluctuation and polluted air parcel influence. (b) Calculate the hour-to-hour changes in CO_2 and retain any two consecutive hourly values where the hour-to-hour difference was <0.5 ppmv (approximately 5% of the raw records removed); selection of relatively well mixed and coincident air parcels. (c) Remove the CO_2 hourly values associated with the NE–ENE and N in summer (approximately 17% removed), NE–ENE–E–ESE in winter (approximately 5% removed) NE–ENE–E in spring (approximately 15% removed), and ENE–E directions in autumn (approximately 10% removed). In addition, remove CO_2 hourly values during calm conditions, or during periods with horizontal wind speed >10 m s^{-1}, or vertical wind speed > ±1 m s^{-1} (approximately 8% of the raw records removed). (d) Remove the hourly concentrations differed from an iterative approach fitting curve (weighted least squares) by >3σ for each

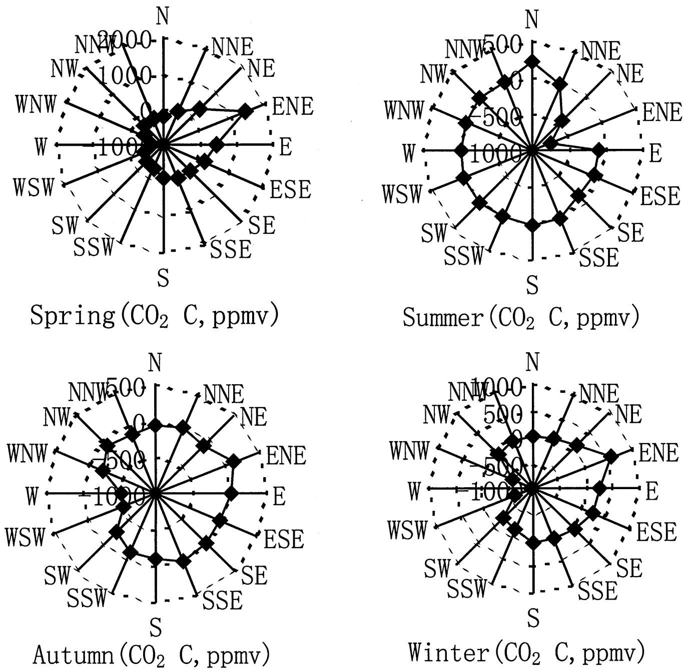

Fig. 6. CO_2 hourly mixing ratios weighted by frequency of wind occurrence in spring, summer, autumn and winter at Mt. Waliguan, 1994–2000.

day using the remaining data (approximately 3% of the raw records removed).

Figure 7 shows all the selected CO_2 hourly data during the period 1994–2000. The selected "baseline" data set account for approximately 70% of the raw hourly records. Daily, monthly and annual means of CO_2 at Mt. Waliguan were computed from the final selected hourly data set.

3.4. *Influence of long-range transport to the observed CO_2 short-term fluctuations*

Lagrangian isobaric back trajectories were calculated for air parcels reaching Waliguan every 6 h (00, 06, 12, 18 UTC) during 1994–1998 at endpoint heights corresponding to 600 mbar levels. The 600 mbar trajectories constitute the main data set used in this

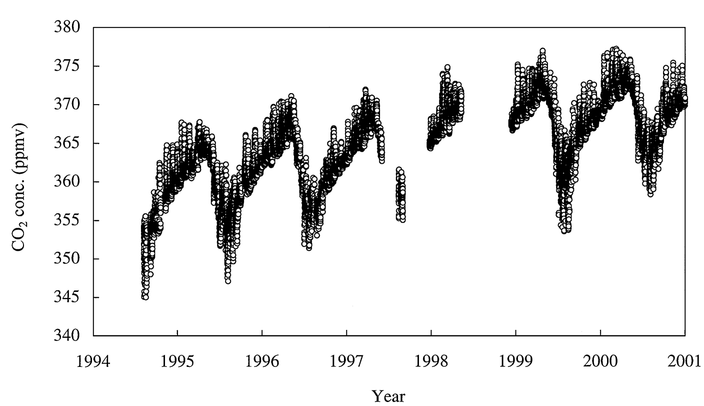

Fig. 7. Selected CO_2 hourly data set at Mt. Waliguan, 1994–2000.

study because they were considered to be the most representive of the air being sampled at Waliguan station. Each trajectory calculation was carried back for 5 d. In general, Waliguan trajectories calculated for pressure levels of 500 and 600 mbar were quite similar (Zhou, 2001a). Accoring to Bridgman and Bodhaine (1994); Halter and Harris (1983) and Worthy et al. (1994), although this time length is unlikely to be sufficient to permit source region identification, air parcel location 5 d previous to arrival at Waliguan can still provide valuable information and indicate a reasonable link to a potential source region.

Figures 8 and 9 show the Waliguan trajectory clusters in the four different seasons during the period 1994–1998. There are 496, 480, 248 and 496 trajectories being selected, in winter, spring, summer and autumn, respectively, according to the calculated trajectories and corresponding CO_2 observed data available at Mt. Waliguan (Zhou, 2001a). The influence of air mass long-range transport on the Waliguan atmospheric CO_2 variation in different seasons was further investigated using the trajectory cluster CO_2 concentration analysis, similar to that used by Brankov et al. (1998), Cape et al. (2000) and Harris (1997), in that CO_2 concentrations are segregated by those closest to each other with similar directions.

Table 1 shows the cluster CO_2 concentrations corresponding to each of the clusters (refer to Fig. 7 for each of cluster sequence and route) in different seasons at Waliguan, centered to zero concentration level

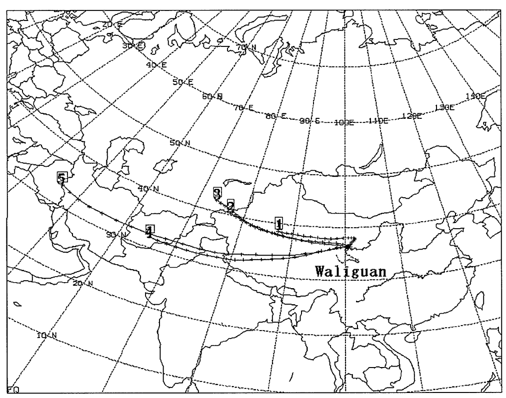

Waliguan 600mb trajectory clusters in winter, 1994-1998

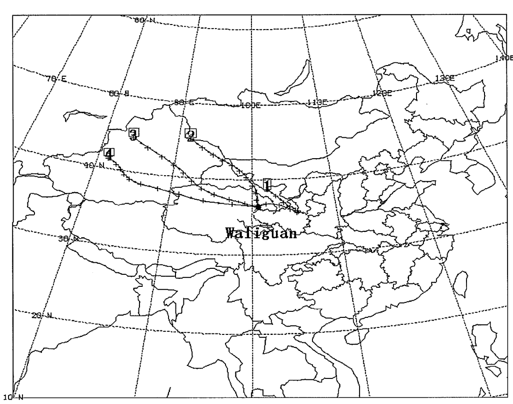

Waliguan 600mb trajectory clusters in spring, 1994-1998

Fig. 8. 600 mbar isobaric trajectory clusters in winter and spring at Mt. Waliguan, 1994–1998. Numbers beside each cluster indicate each of the cluster sequences (as indicated in Table 2).

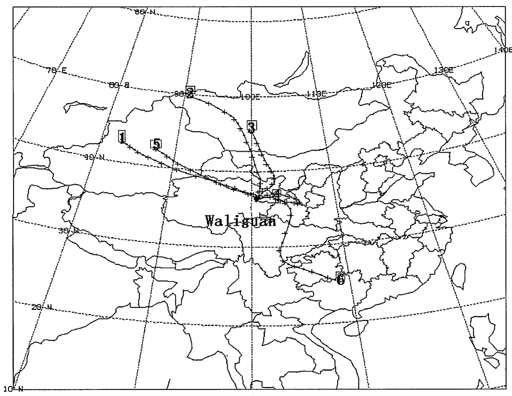

Waliguan 600mb trajectory clusters in summer, 1994-1998

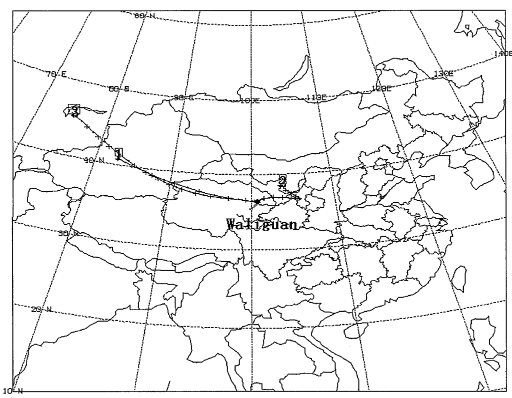

Fig. 9. 600 mbar isobaric trajectory clusters in summer and autumn at Mt. Waliguan, 1994–1998. Numbers beside each cluster indicate each cluster sequence (as indicated in Table 2).

Table 1. *Cluster CO_2 concentration (conc. ppmv) centered at zero level in spring, summer autumn and winter at Mt. Waliguan, 1994–1998*

Cluster	Winter		Spring		Summer		Autumn	
serial number (refer to Fig. 8)	Trajec. count	Conc. (ppmv)	Trajec. count	Conc. (ppmv)	Trajec. count	Conc. (ppmv)	Trajec. count	Conc. (ppmv)
1	56	1.81	96	4.34	60	−4.63	266	−3.54
2	142	0.22	115	3.81	54	−6.59	86	−3.30
3	159	−0.04	148	3.16	40	−6.34	144	−3.73
4	95	−0.02	121	3.02	54	−6.81		
5	44	0.04			25	−5.51		
6					15	−5.08		
Total	496		480		248		496	

The ‘Cluster serial number’ indicates each cluster relevant to different air parcel origin/routes displayed in Figure 8. It is also associated with each of the cluster CO_2 concentration in different seasons showed in this table, abbreviated as ‘conc. (ppmv)’.‘Trajec. count’ represents quantity of trajectories hold similar directions in each corresponding cluster.

for comparison. Each cluster CO_2 concentration was calculated by the equation:

$$[\text{cluster } CO_2 \text{ concentrations}] = [\text{trajectory } CO_2 \text{ concentration}]_i / n$$

Where the [trajectory CO_2 concentration]$_i$ is the observed CO_2 mixing ratio corresponding to the trajectory (i) arrival time, where i represents the sequence number of a trajectory (one of the trajectories held with similar directions) in an individual cluster, and n is the total number of trajectories in this cluster.

Figures 8 and 9 and Table 1 indicated that the highest cluster CO_2 concentration is associated with cluster 1 in winter, which passes through the north-eastern industrial and populated area. The elevated cluster CO_2 concentration is associated with cluster 1 and cluster 2 in spring, and cluster 1 in autumn, which mostly come from the NE–ENE–E sector. In summer, however, the decreased cluster CO_2 concentration most likely corresponds to an air parcel coming from the NE–ENE–E sector and N direction. Considering CO_2 sources, sinks and long-range transport in different seasons investigated by other researchers (Chung, 1988; Colombo et al., 2000; Denning et al., 1995; Harris, 1992; 1997; Higuchi et al., 1987; Higuchi and Daggupaty, 1985; Pearman, 1977; Pearman and Hyson, 1980), and combining the estimated $1^\circ \times 1^\circ$ latitude–longitude resolution grid map of CO_2 emissions over continental China (Bai, 1996) with each back-trajectory cluster route at Waliguan in Fig. 8, it should be noted that eastern China has become one of the highest emission regions in Asia due to rapid growth both in economy and population in the past decades; however, emissions in western China have consistently been lower. The results and discussion suggest that air parcels originating from NE–ENE–E in all seasons and additionally the N direction (with more vegetation) in summer cause considerable short-term variation in the Waliguan CO_2 records.

3.5. *Atmospheric CO_2 background characteristics*

Figure 10 shows the averaged diurnal variation of atmospheric CO_2 in different seasons at Waliguan during the period 1994–2000, with the standard deviation of the hourly mean indicated as an error bar. The diurnal variation in summer is much more significant (up to 2 ppmv) than during the other three seasons (less than 0.5 ppmv). This is primarily due to nighttime respiration and daytime photosynthesis. As mentioned earlier, the winter period variability is mainly due to the transport from anthropogenic regions on timescales seen in the synoptic variability.

Based on selected CO_2 hourly data, statistical analysis shows the distribution of CO_2 mixing ratios during the period 1994–2000 to be 364–374, 354–370, 356–368 and 362–372 ppmv (with >90% occurrence) in spring, summer, autumn and winter, respectively. Figure 11 shows CO_2 monthly mean time series at Waliguan during the period 1994–2000, with standard deviation indicated as an error bar. This reflects the exchange activities between the atmosphere and terrestrial ecosystem in the middle–high latitudes of the Northern Hemisphere (NH). Inter-annual variability in the seasonal cycle is due to variation in the balance between photosynthesis and respiration, as well

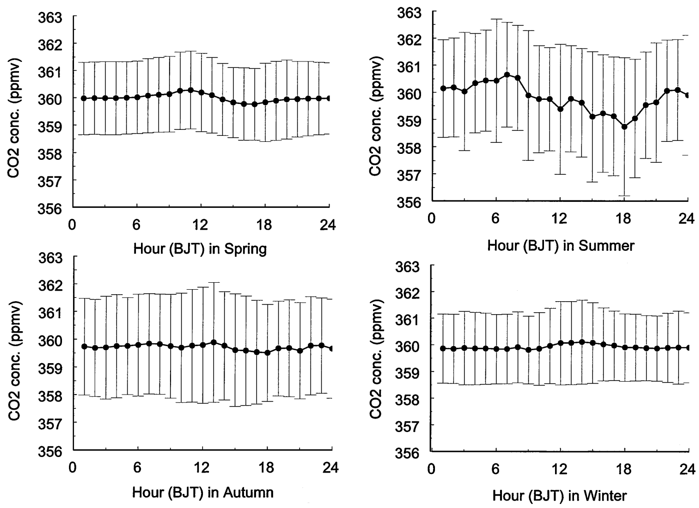

Fig. 10. Averaged CO_2 diurnal variations in spring, summer, autumn and winter at Mt. Waliguan, with standard deviations indicated as error bars, 1994–2000. Hour (BJT) = UTC + 8 h = Waliguan Local Time + 1 h.

as ocean uptake and release. The strong seasonality in the NH is due to photosynthesis and respiration of the terrestrial biosphere; seasonality in the Southern Hemisphere, however, is much smaller and opposite in phase. The study of longer-time atmospheric CO_2 monitoring records (Bacastow et al., 1985; Tans et al., 2001) showed that CO_2 seasonal amplitude of the NH was enhanced in past decades. This phenomenon, however, is hardly distinguished in Waliguan CO_2 records during the period 1994–2000.

Figure 12 shows the CO_2 averaged seasonal cycle by detrended "baseline" data at Waliguan during the period 1994–2000, with standard deviation indicated as an error bar, in which the estimated long-term trend (12 months running mean, similar to the method in Conway et al., 1994) is removed at first. There was an obvious seasonal cycle, with a maximum occurring in April and a minimum in August, CO_2 mixing ratios declining rapidly during the period May–July but climbing fleetly during the period September–November.

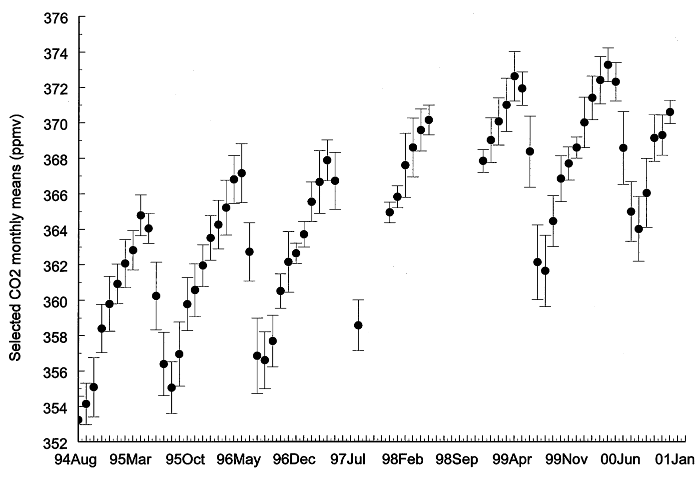

Fig. 11. CO_2 monthly mean time series based on selected hourly records at Waliguan, with standard deviations indicated as error bars, 1994–2000.

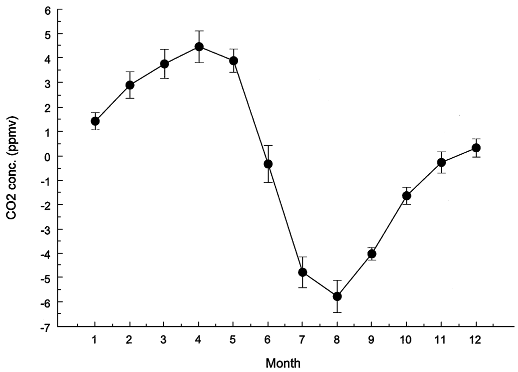

Fig. 12. CO_2 averaged seasonal cycle at Mt. Waliguan, with standard deviation indicated as error bars, 1994–2000.

The averaged CO_2 seasonal amplitude was up to 10.5 ppmv, which reflects the periodicity of terrestrial vegetation growth (the metabolic cycle of the land biota) in the middle to high latitudes of the NH. In comparison with some literature results (Masarie and Tans, 1995; Tans et al., 2001; WMO, 2000), the temporal phase of the Waliguan CO_2 seasonal cycle almost agrees with the records from other WMO/GAW baseline stations Alert (82°26′N, 62°30′W, 210 m asl), Barrow (71°19′N, 156°36′W, 11 m asl), Mace Head (53°19′N, 9°53′W, 25 m asl) and Zugspitze (47°25′N, 10°59′E, 2960 m asl), and regional stations Ulaan Uul (44°27′N, 111°06′E, 914 m asl), Niwot Ridge (40°3′N, 105°35′W, 3475 m asl), Ryori (39°2′N, 141°50′E, 230 m asl) and Tae-ahn Peninsula (36°44′N, 126°8′E, 20 m asl)], all of which are located in the middle to high latitudes of the NH. It is, however, about one month earlier than that of lower latitudinal baseline stations Izana (28°18′N, 16°29′W, 2367 m asl), Minamitorishima (24°18′N, 153°58′E, 8 m asl) and Mauna Loa (19°32′N, 155°35′W, 3397 m asl), due to different CO_2 sources and sinks from land or ocean. The Waliguan CO_2 seasonal amplitude also comes within the range of middle to high latitudes in the NH, in which the approximate seasonal amplitudes of the above mentioned monitoring stations are as follows: Alert (14 ppmv), Barrow (18 ppmv), Mace Head (14 ppmv), Zugspitze (15 ppmv), Ulaan Uul (17 ppmv), Niwot Ridge (11 ppmv), Ryori (13 ppmv), Tae-ahn Peninsula (15 ppmv), Izana (8 ppmv), Minamitorishima (9 ppmv) and Mauna Loa (8 ppmv). It can be seen that the amplitudes of the CO_2 seasonal cycle are clearly large in northern high and mid-latitudes but small in low latitudes.

Table 2 provides CO_2 annual means and growth rates at Waliguan during the period 1991–2000, as well as records of some other monitoring stations located in a similar latitudinal band (http://cmdl.noaa.gov/ccgg). The Waliguan annual means are merged from all of the selected records of in-situ NDIR and GC-FID observations, as well as cooperative flask air sampling results once per week since 1991, analyzed by NOAA/CMDL (Zhou et al., 1998b; Zhou, 2001). The Waliguan CO_2 annual means show an approximately linear increase with averaged growth rate of approximately 1.6 ppmv yr^{-1} during the period 1991–2000. However, the growth rates vary significantly inter-annually, from the lowest value 0.7 ppm in 1992 to the highest value around 2 ppmv in 1997–1998. According to literature results (Colombo et al., 2000; Masarie and Tans, 1995; Tans et al., 2001; WMO, 2000), the global annual mean CO_2 mixing ratio is 355 ppmv (1992), 359.7 ppmv (1995), 363 ppmv (1997) and 369 ppmv (2000), respectively, 3–4 ppm higher in the NH where anthropogenic emissions are greatest, with a global growth rate of 1.5 ppmv yr^{-1} on average for the period 1983–2000. The CO_2 concentration peak in northern high and mid-latitudes reflects strong net sources in these areas. The high global growth rates in 1983, 1987/1988, 1994/1995, and 1997 are associated with warm El Niño Southern (ENSO) events; the anomalously strong El Niño event in 1997/1998 brought about record-breaking high increases in 1997/1998 (WMO, 2000; Watanabe et al., 2000). The exceptional low growth rate in 1992, however, was caused by low global air temperatures following the eruption of Mt. Pinatubo in 1991 (Conway et al., 1994). Based on the above results and discussions, we concluded that Waliguan CO_2 annual means and growth rates coincide with most of the published results of baseline monitoring stations in NH, and can further support the well known argument of the world-wide influence of fossil-fuel emissions on the atmosphere.

4. Conclusions

The horizontal wind direction of NE–ENE–E in all seasons, appended with the N direction in summer, was the major non-background section of atmospheric CO_2 observations at Mt. Waliguan. Horizontal wind speeds > 10 m s^{-1}, calm conditions, or vertical wind speeds $> \pm 1$ m s^{-1} in all seasons have a maximum impact on CO_2 hourly mixing ratios, depending on different origins and routes of air flow arriving at the Waliguan sampling site. A background data

Table 2. *Atmospheric CO_2 annual means (ppmv) and growth rates (ppmv) at Waliguan and other Northern Hemisphere stations, 1991–2000*

Year	1991	1992	1993	1994	1995	1996	1997	1998	1999	2000
Waliguan										
Annual mean	355.2	356.7	357.4	359.2	360.6	362.2	363.8	365.9	367.9	369.5
Growth rate	1.5	0.7	1.8	1.4	1.6	1.6	2.1	2.0	1.6	
Barrow										
Annual mean	357.6	357.5	358.2	359.6	361.9	364.1	365.0	367.4	369.8	
Growth rate	−0.1	0.7	1.4	2.3	2.2	0.9	2.4	2.4		
Mace Head										
Annual mean		356.1	356.7	358.6	360.8	363.1	364.3	366.3	368.4	
Growth rate		0.6	1.9	2.2	2.3	1.2	2.0	2.1		
Ulaan Unl										
Annual mean		356.6	357.1	359.3	360.8	362.4	363.7	367.5	368.7	
Growth rate		0.5	2.2	1.5	1.6	1.3	3.8	1.2		
Niwot Ridge										
Annual mean	356.1	356.9	357.4	359.5	361.2	363.0	363.9	366.5	368.4	
Growth rate	0.8	0.5	2.1	1.7	1.8	0.9	2.6	1.9		
Tae-ahn										
Annual mean	359.7	360.5	360.4	361.2	364.0	366.3	368.7	370.6	373.1	
Growth rate	0.8	−0.1	0.8	2.8	2.3	2.4	1.9	2.5		
Izana										
Annual mean		356.2	357.5	358.6	361.5	363.0	363.7	367.1	368.5	
Growth rate		1.3	1.1	2.9	1.5	0.7	3.4	1.4		
Mauna Loa										
Annual mean	355.6	356.5	356.9	358.5	360.6	362.4	363.5	366.6	368.2	
Growth rate	0.9	0.4	1.6	2.1	1.8	1.1	3.1	1.6		

selection procedure was suggested according to statistical analysis and influence of local surface winds, with a selected hourly data set that represents “baseline” conditions accounting for approximately 70% of the raw records. Air parcel long-range transport coming from the NE–ENE–E in all seasons, appended with the N direction in summer, brought about considerable CO_2 short-term variation. The CO_2 diurnal variation in summer is much more significant than in the other three seasons, representing vegetation and soil microbe activities at the sampling site. From a selected “baseline” hourly data set, distribution of CO_2 mixing ratios in different seasons and CO_2 monthly mean time series reflected exchanges between the atmosphere and terrestrial ecosystem in the middle to high latitudes of the NH. The averaged CO_2 seasonal cycle, as well as CO_2 annual means and growth rates, coincided with most of the records obtained from other WMO/GAW or NOAA/CMDL monitoring stations located in a similar latitudinal band. The highly quality-controlled CO_2 monitoring system and data set at Waliguan can be used in modeling and other studies to improve our understanding of carbon source and sink distributions, particularly over the Asian continent. The Waliguan CO_2 records are regularly submitted to the WMO World Data Center for Greenhouse Gases (WDCGG, http://gaw.kishou.go.jp/wdcgg.html), and are also integrated into the Cooperative Atmospheric Data Integration Project (CADIP, anonymous FTP to ftp.cmdl.noaa.gov/ccgg/co2/globalview).

5. Acknowledgments

We thank the staff of the Waliguan Station for their diligent efforts in operating the CO_2, surface wind and other baseline observing systems. We also appreciate the WMO/Environment Division for the coordination of the GAW programme, Canada/MSC for cooperation with the Waliguan GC-FID program and also providing trajectories, NOAA/CMDL for cooperation with the Waliguan NDIR and flask air sampling program, and NOAA/ARL for providing the trajectory cluster program. This work was supported by the United Nations GEF Fund (GLO/91/G32), the China Ministry of Science and Technology project (G99-A-07) and a Japan Society for Promotion of Science post-doctorial fellowship (PB01736).

REFERENCES

Bacastow, R. B., Keeling, C. D. and Whorf T. P. 1985. Seasonal amplitude increase in atmospheric CO_2 concentration at Mauna Loa, Hawii, 1959–1982. *J. Geophys. Res*. **90**, 10 529–10 540.

Bai, N. B. 1996. Estimation of emissions of CO_2, SO_2 and NO_x per $1^\circ \times 1^\circ$ grid square in China in 1992. In:*Atmospheric ozone variation and its impact on the climate and environment over China*, (ed. X. J. Zhou). Meteorological Press, Beijing, 145–150.

Beardsmore, D. J. and Pearman, G. I. 1987. Atmospheric carbon dioxide measurements in the Australian region: data from surface observatries. *Tellus* **39B**, 42–66.

Brankov, E., Rao, S. T. and Porter, P. S. 1998. A trajectory-clustering-correlation methodology for examining the long-range transport of air pollutants. *Atmos. Environ*. **32**, 1525–1534.

Bridgman, H. A. and Bodhaine, B. A. 1994. On the frequency of long-range transport events at Point Barrow, Alaska, 1983–1992. *Atmos. Environ*. **28**, 3537–3549.

Cape, J. N., Methven, J. and Hudson, L. E. 2000. The use of trajectory cluster analysis to interpret trace gas measurements at Mace Head, Ireland. *Atmos. Environ*. **34**, 351–363.

Chung, Y. S. 1988. The variations of atmospheric carbon dioxide at Alert and Sable Island, Canada. *Atmos. Environ*. **22**, 383–394.

Ciattaglia, L. 1983. Interpretation of atmospheric CO_2 measurements at Mt. Cimone (Italy) related to wind data. *J. Geophys. Res*. **88**, 1331–1338.

Ciattaglia, L., Cundari, V. and Colombo, T. 1987. Further measurements of atmospheric carbon dioxide at Mt. Cimone, Italy: 1979–1985. *Tellus* **39B**, 13–20.

Ciattaglia, L., Colombo, T. and Masarie, K. A. 1999. Continuous measurements of atmospheric CO_2 at Jubany station, Antarctica. *Tellus* **51B**, 713–721.

Colombo, T., Santaguida, R., Capasso, A., Calzolari, F., Evangelisti, F. and Bonasoni, P. 2000. Biospheric influence on carbon dioxide measurements in Italy. *Atmos. Environ*. **34**, 4963–4969.

Conway, T. J. and Steele, L. P. 1989. Carbon dioxide and methane in the Arctic atmosphere. *J. Atmos. Chem*. **9**, 81–100.

Conway, T. J., Steele, L. P. and Novelli, P. C. 1993. Correlations among atmospheric CO_2, CH_4 and CO in the Arctic, March 1989. *Atmos. Environ*. **27A**, 2881–2894.

Conway, T. J., Tans, P. P., Waterman, L. S., Thoning, K. W., Kitzis, D. R., Masarie, K. A. and Zhang, N. 1994. Evidence for international variability of the carbon cycle from the NOAA/CMDL Global Air Sampling Network. *J. Geophys. Res*. **99**, 22 831–22 855.

Denning, A. S., Fung, I. Y. and Randall, D. 1995. Latitudinal gradient of atmospheric CO2 due to seasonal exchange with land biota. *Nature* **376**, 240–243.

Gaudry, A., Ascencio J. M. and Lambert, G. 1983. Preliminary study of CO_2 variations at Amsterdam Island. *J. Geophys. Res*. **88**, 1323–1329.

Gaudry, A., Monfray, P., Polian, G., Bonsang, G., Ardouin, B., Jegou, A. and Lambert, G. 1991. Non-seasonal variations of atmospheric CO_2 concentrations at Amsterdam Island. *Tellus* **43B**, 136–143.

Gras, J. L. 2001. Aerosol black carbon at Cape Grim, by light absorbtion. In: *Baseline Atmospheric Program Australia 1997–98* (ed. N. W. Tindale, N. Derek and R. J. Francey). Bureau of Meteorology and CSIRO Atmospheric Research, Melbourne, Australia, 20–26.

Halter, B. and Harris, J. M. 1983. On the variability of atmospheric carbon dioxide concentration at Barrow, Alaska during winter. *J. Geophys. Res*. **88**, 6858–6864.

Halter, B. C., Harris, J. M. and Conway, T. J. 1988. Component signals in the record of atmospheric carbon dioxide concentration at American Samoa. *J. Geophys. Res*. **93**, 15 914–15 918.

Hansen, A. D. A., Conway, T. J., Steele, L. P., Bodhaine, B. A., Thoning, K. W., Tans, P. P. and Novakov, T. 1989. Correlation among combustion effluent species at Barrow, Alaska: Aerosol black carbon, carbon dioxide, and methane. *J. Atmos. Chem*. **9**, 283–299.

Harris, J. M. 1992. An analysis of 5-day mid-tropospheric flow patterns for the South Pole: 1985–1989. *Tellus* **44B**, 409–421.

Harris, J. M. 1997. 10 years trajectories and cluster analysis. *J. Geophys. Res*. **102**, 8781–8791.

Harris, J. M. and Kahl, J. D. 1990. A discriptive atmospheric transport climatology for the Mauna Loa Observatory, using clustered trajectories. *J. Geophys. Res*. **95**, 13 651–13 667.

Haszpra, L. 1999. On the representativeness of carbon dioxide measurements. *J. Geophys. Res*. **104**, 26 953–26 960.

Higuchi, K. and Daggupaty, S. M. 1985. On variability of atmospheric CO_2 at Station Alert. *Atmos. Environ*. **19**, 2039–2044.

Higuchi, K., Trivett, N. B. A. and Daggupaty, S. M. 1987. A preliminary climatology of trajectories related to atmospheric CO_2 measurements at Alert and Mould Bay. *Atmos. Environ*. **21**, 1915–1926.

Hopper, J. F., Worthy, D. E. J., Barrie, L. A. and Trivett, N. B. A. 1994. Atmospheric observations of aerosol black carbon, carbon dioxide, and methane in the high arctic. *Atmos. Environ*. **28**, 3047–3054.

Keeling, C. D., Bacastow, R. B., Bainbridge, A. E., Ekdahl, C. A. Jr., Guenther, P. R. and Waterman, L. S. 1976a. Atmospheric carbon dioxide variations at Mauna Loa Observatory, Hawaii. *Tellus* **28**, 538–551.

Keeling, C. D., Adams, J. A. Jr., Ekdahl, C. A. Jr. and Guenther, P. R. 1976b. Atmospheric CO_2 variations at the South Pole. *Tellus* **28**, 552–564.

Masarie, K. A. and Tans, P. P. 1995. Extension and integration of atmospheric carbon dioxide data into a globally consistent measurement record. *J. Geophys. Res*. **100**, 11 593–11 610.

Navascues, B. and Rus, C. 1991. Carbon dioxide observations at Izana baseline station, Tenerife (Canary Islands): 1984–1988. *Tellus* **43B**, 118–125.

Pearman, G. I. 1977. Further studies of the comparability of baseline atmospheric carbon dioxide measurements. *Tellus* **29**, 171–181.

Pearman, G. I. and Hyson, P. 1980. Activities of the global biosphere as reflected in atmospheric CO_2 records. *J. Geophys. Res*. **85**, 4468–4474.

Peterson, J. T. 1999. Carbon dioxide round robin reference gas intercomparison. In: *Report of the 9th WMO meeting of experts on CO_2 concentration and related tracer measurement techniques*. Aspendale, Victoria, Australia, 1997. (ed. R. J., Francey). WMO, Geneva, Switzerland,30–33.

Tang, J., Wen, Y. P., Xu, X. B., Zheng, X. D., Guo, S. and Zhao, Y. C. 1995. China Global Atmosphere Watch Baseline Observatory and its measurement program. In: *CAMS Annual Report 1994–95*. China Meteorological Press, Beijing, 56–65.

Tang, J., Wen, Y. P., Zhou, L. X., Qi, D. L., Zheng, M., Trivett, N. B. A. and Wallgren, E. 1999. Study of black carbon aerosol in western China. *Chin. Q. J. Appl. Meteorol*. **9**, 160–170.

Tans, P. P., Bakwin, L., Bruhwiler, L., Conway, T. J., Dlugokencky, E. J., Guenther, D. W., Kitzis, D. R., Lang, P. M., Masarie, K. A., Miller, J. B., Novelli, P. C., Thoning, K. W., Trudeau, M., Vaughn, B. H., White, J. W. C. and Zhao, C. 2001. 2. Carbon cycle. In: *Climate Monitoring and Diagnostics Laboratory Summary Report No. 25*, 1998–1999 (eds. R. C. Russel, D. B. King and R. M. Rosson),Boulder, Colorado, USA, 24–46.

Thoning, K., Tans, P. P. and Komhyr, W. D. 1989. Atmospheric carbon dioxide at Mauna Loa observatory, 2: Analysis of the NOAA GMCC data, 1974–1985. *J. Geophys. Res*. **94**, 8549–8565.

Watanabe, F., Uchino, O., Joo, Y., Aono, M., Higashijima, K., Hirano, Y., Tsuboi, K. and Suda, K. 2000. Interannual variation of growth rate of atmospheric carbon dioxide concentration observed at the JMA's three monitoring stations: large increase in concentration of atmospheric carbon dioxide in 1998. *J. Meteorol. Soc. Jpn*. **78**, 673–682.

Waterman, L. S., Nelson, D. W., Komhyr, W. D. and Harris, T. B. 1989. Atmospheric carbon dioxide measurements at Cape Matatula, American Samoa, 1976–1987. *J. Geophys. Res*. **94**, 14 817–14 829.

Wen, Y. P., Shao, Z. Q., Xu, X. B., Ji, B. F. and Zhu, Q. B. 1994. Observation and investigation of variabilities of baseline CO_2 concentration over Waliguan Mountain in Qinghai Province of China. *Acta Meteorol. Sin*. **8**, 255–262.

WMO. 1978. *International operations handbook for measurement of background atmospheric pollution*. WMO, No. 491. Geneva, Switzerland.

WMO. 1981. *Report of WMO/UNEP/ICSU meeting on instruments, standardization and measurements techniques for atmospheric CO_2*. WMO, Geneva, Switzerland, 8–11, Septmber 1981.

WMO. 1993. *Global atmosphere watch measurement guide*. No. 143. (WMO TD No. 1073), Geneva, Switzerland.

WMO. 1997. *Report of the 9th WMO meeting of experts on CO_2 concentration and related tracer measurement techniques* (ed. R. Francey). No. 132, TD-No. 952. Aspendale, Victoria, Australia. 1–4 September 1997.

WMO. 2000. *World Data Center for Greenhouse Gases (WDCGG) Data Summary*. WDCGG No. 22. Tokyo, Japan.

WMO. 2001. *Strategy for the Implementation of the Global Atmosphere Watch Programme (2001-2007), a contribution to the implementation of the WMO long-term plan*. No. 142, WMO, Geneva, Switzerland, June 2001.

Worthy, D. E. J., Trivett, N. B. A., Hopper, J. F., Bottenheim, J. W. and Levin, I. 1994. Analysis of long-range transport events at Alert, Northwest Territories, during the polar sunrise experiment. *J. Geophys. Res*. **99**, 25 329–25 344.

Zhou, L. X. 2001. Study on the background characteristics of major greenhouse gases over continental China. Ph.D. Dissertation, Peking University, China.

Zhou, L. X., Tang, J., Zhang, X. C., Ji, J., Wang, Z. B., Worthy, D., Emst, M. and Trivett, N. B. A. 1998a. In-situ gas chromatographic measurement of atmospheric methane and carbon dioxide. *Acta Sci. Circumstantia* **18**, 356–361.

Zhou, L. X., Tang, J., Wen, Y. P., Zhang, X. C., Ji, J., Zheng, M., Worthy, D., Trivett, N. B. A., Tans, P. P. and Conway, T. 1998b. Characteristics of atmospheric methane concentration variation at Mt. Waliguan. *Q. J. Appli. Meteorol*. **9**, 385–391.

Zhou, L. X., Tang, J., Ernst, M. and Worthy, D. 2001. Continuous measurement of baseline atmospheric carbon monoxide in western china. *Environ. Sci*. **22**, 1–5.